

Crops and Soils Research Paper

Cite this article: González JA, Mercado MI, Martínez-Calsina L, Erazzú LE, Buedo SE, González DA, Ponessa GI (2022). Plant density effects on quinoa yield, leaf anatomy, ultrastructure and gas exchange. *The Journal of Agricultural Science* **160**, 349–359. <https://doi.org/10.1017/S0021859622000533>

Received: 5 June 2022

Revised: 22 July 2022

Accepted: 20 August 2022

First published online: 25 August 2022

Key words:

Argentina; chloroplast; leaf anatomy; light competition; photosynthesis

Author for correspondence:

M. I. Mercado, E-mail: mimercado@lillo.org.ar

Plant density effects on quinoa yield, leaf anatomy, ultrastructure and gas exchange

J. A. González¹ , M. I. Mercado² , L. Martínez-Calsina^{3,4}, L. E. Erazzú^{3,4}, S. E. Buedo¹, D. A. González⁵ and G. I. Ponessa²

¹Instituto de Ecología, Comportamiento y Conservación, Fundación Miguel Lillo, Miguel Lillo 251, Tucumán, Argentina; ²Instituto de Morfología Vegetal, Fundación Miguel Lillo, Miguel Lillo 251, Tucumán, Argentina;

³Famaillá, Instituto Nacional de Tecnología Agropecuaria (INTA), Tucumán, Argentina; ⁴Facultad de Agronomía y Zootecnia, Universidad Nacional de Tucumán, Tucumán, Argentina and ⁵Instituto de Bioprospección y Fisiología Vegetal (INBIOFIV), CONICET-UNT; Facultad de Ciencias Naturales e Instituto Miguel Lillo, Tucumán, Argentina

Abstract

To study the impact of plant density on *Chenopodium quinoa* (c.v. CICA-17) achene yield and its relationship with morphology, leaf anatomy and gas exchange in the absence of water stress, field trials were conducted at 1995 m asl in Northwestern Argentina. Two plant densities were evaluated; low density (LD) 7.2 plants/m ($120\ 240\ \text{pl}/\text{ha}$) and high density (HD) 27.9 plants/m ($465\ 930\ \text{pl}/\text{ha}$). HD treatment caused light competition, inducing morphological and anatomical changes in Quinoa plants. Plants grown under HD conditions showed decreases in plant height and stem diameter, lower stomatal dimensions and densities, and thinner leaf blades. Compensation strategies such as increases in specific leaf area and a higher number chloroplasts per palisade cell were observed, nevertheless these changes did not fully compensate C absorption and gas exchange limitations, therefore limiting the uptake of N and P and resulting in a 53.2% lower yield of HD compared to LD. Considering the ability of quinoa plants to change its morphology and anatomy, further studies with intermediate plant densities are necessary in order to determine if it is possible to achieve higher yields and to increase the efficiency in the use of the resources.

Introduction

Quinoa (*Chenopodium quinoa* Willd.) is an Andean crop with a great world attention (Bazile *et al.*, 2016a, 2016b) for its extraordinary nutritional properties (Bazile *et al.*, 2015; González *et al.*, 2015) and for its potential as an industrial crop, i.e. quinoa starch can be used to stabilize emulsions (Rayner *et al.*, 2012), quinoa flour was proposed as ingredient for meat burger instead of soybean flour to get better and more healthy products (Shokry, 2016), to obtain saponins with potential application in the food, cosmetics, agricultural and pharmaceutical industries (El Hazzam *et al.*, 2020), among other uses. This species is also useful as fodder (González *et al.*, 2016; Asher *et al.*, 2020) or in decontamination processes (Thomas and Lavkulich, 2015; Shabbir *et al.*, 2021). Due to its outstanding plasticity, quinoa constitutes an alternative crop capable of adapting to the climate change scenarios (Ruiz *et al.*, 2014; Alandia *et al.*, 2020; Andreotti *et al.*, 2022). In recent years, this crop has undergone a major expansion. Selected quinoa genotypes were evaluated and successfully cultivated under different environments outside the Andean region with the aim to strengthen food and nutrition security (Bazile *et al.*, 2016a, 2016b; Alandia *et al.*, 2020; Angeli *et al.*, 2020; Asher *et al.*, 2020; Hinojosa *et al.*, 2021).

Thus, quinoa is unequivocally a multipurpose species. Nowadays farmers interested in achene production are trying to manage quinoa crop in order to obtain a higher achene yield. Hence, several quinoa crop field trials tested different agricultural management practices, such as reduced row spacing and higher plant densities, looking for a yield improvement (Jacobsen and Christiansen, 2016; Abdalla *et al.*, 2020).

Plant density affects plants morphology and productivity. These effects can be explained by water, nutrients (Villalobos *et al.*, 2016), radiation (Hodgson and Blackman, 1957; Heitholt and Sassenrath, 2010) and CO₂ competition (Van Kleunen *et al.*, 2006) among plants (Lambers *et al.*, 1998). This adaptation implies increases in stem elongation and changes in stem orientation, also changes in number and architecture of the branches to achieve different exposition to solar radiation, among others. Jacobsen (2015) showed that quinoa at low densities has the ability to compensate the empty spaces between plants by changes in its morphology. An increase of the branching system in quinoa under low plant density was also reported by Spehar and da Silva Rocha (2009) and Abdalla *et al.* (2020). Several authors (Jacobsen *et al.*, 1994; Ruiz and Bertero, 2008; Spehar and da Silva Rocha, 2009; Eisa *et al.*, 2018; Abdalla *et al.*, 2020; Parwada *et al.*, 2020; Cruz Díaz *et al.*, 2021) around the world

(Denmark, Argentina, Brazil, Egypt, Burkina Faso, Zimbabwe and Colombia) studied the effect of plant density on quinoa yield. Except for Jacobsen *et al.* (1994) and Ruiz and Bertero (2008) who found higher yields increasing plant density; the other researchers found higher yields at lower plant densities. It is worth noting that the researchers above mentioned studied a wide range of plant densities (22 000–600 000 plants per hectare) in different environments.

However, none of the reviewed studies reports on the possible causes that may have generated this drop in yield. Different plant densities and light competition produce changes in leaf anatomy and chloroplast ultrastructure affecting in turn the photosynthetic assimilation rates and productivity (Miltphore *et al.*, 1982; Feng *et al.*, 2018). Chloroplasts are the main photosynthetic organelle. Decrease in the number of chloroplasts or changes in its structure led to the decrease of photosynthetic pigments, resulting in the decline of net photosynthetic rate and reduced yield (Ren *et al.*, 2017).

Until now, photosynthetic studies in quinoa were limited to gas exchange and its relation with different abiotic stresses (González *et al.*, 2011, 2014, 2019; Eustis *et al.*, 2020; Delatorre-Herrera *et al.*, 2021) and very scarce investigations were related to leaf anatomy and chloroplast ultrastructure (González *et al.*, 2014; Manaa *et al.*, 2019).

To understand quinoa yield under different conditions and its extraordinary adaptation to diverse environments, studies relating photosynthesis process with physiology, morphology, leaf structure and ultrastructure are necessary. This kind of investigations are necessary to get a more complete knowledge in relation to quinoa plasticity and to achieve a better understanding of the behaviour of quinoa ecotypes in different environments around the world where this crop is being evaluated as alternative. Thus, the objective of the present research is to analyse under controlled field conditions the effect of different plant densities on quinoa plant morphology, achene yield, leaves anatomy and ultrastructure in terms of chloroplast organization, and how it affects the physiology in relation to photosynthetic assimilation.

Materials and methods

Experimental site

Field trials were carried out in an arid mountain region of Northwestern Argentina (Encalilla, Amaicha del Valle, 22° 31'S, 65° 59'W, 1995 m asl, Tucumán, Argentina). Climatic classification, according to Köppen, is desert type (BWkaw). Daily average air temperatures were $27.3 \pm 1.4^\circ\text{C}$ (maximum) and $14.1 \pm 1.2^\circ\text{C}$ (minimum) and wind velocity ranged from 10 to 15 km/h, whereas the average of relative humidity (RH, %) was $33.2 \pm 4.1\%$ (González *et al.*, 2011). The soil is a sandy-clay-loam (organic matter content 0.60%, total nitrogen content of 0.55% and a pH 8.8 and electrical conductivity 2.0 dS/m) with a depth of about 0.5 m (González *et al.*, 2011). The soil contains sand (48%), silt (22%) and clay (30%). Na^+ is the first exchangeable (615.2 mg/kg) followed by K^+ (390.2 mg/kg) and Mg^{2+} (342.7 mg/kg). Annual rainfall is 200 mm, with more than 70% occurring between September and February.

Plant material

Chenopodium quinoa Willd. CICA-17 variety was used. CICA-17 is a Peruvian variety obtained from Amarilla de Marangani (A. Mújica-Sánchez, personal communication, 2016) and it was

grown and adapted for the last 15 years in Encalilla site. According to previous results in our experimental field, CICA-17 showed a life cycle of approximately 150–160 days after sowing, adult plants exhibited an average height between 1.50 and 2.5 m, yellow seeds, high assimilation rates ($>30 \mu\text{mol}/\text{m}^2/\text{s}$) and yielding of near 2.3 Tn/ha (González *et al.*, 2011).

Experimental design

Treatments (two plant densities) were arranged in a randomized complete block design with three replicates. Sowing date was on mid-November for both years, 2018 and 2019. Each plot (10×5 m) had five rows (5 m long) with a distance between rows of 0.60 m. Plots were irrigated 24 h before sowing to ensure a good humidity in the soil profile. Hand sowing was performed using a steady flow method. When seedlings had 4–6 leaves, a hand-thinning was carried out to get target plant (pl) densities: $7.2 (\pm 1.0) \text{ pl/m}$ (LD: low density, representing 120 240 pl/ha) and $27.9 (\pm 3.0) \text{ pl/m}$ (HD: high density, representing 465 930 pl/ha). Target plant densities studied here were selected as intermediate in relation to other published works, higher than the lowest density studied (22 000 pl/ha, Ruiz and Bertero, 2008) and lower than the highest studied with other varieties (600 000 pl/ha, Spehar and da Silva Rocha, 2009).

During both crop cycles (2018/2019 and 2019/2020), plants were irrigated with a drip irrigation system three times a week during the first month and weekly until achene filling stage (800 mm of applied water by crop cycle). The irrigation system was designed in order to ensure no water limitations and twice a week visual observations of plant guttation were done to confirm it. Crops did not show any visible water and/or nutrient limitation during both cycles and were kept free of pests and diseases.

Morphological studies

Plant height (m) and stem diameter (cm) were measured on selected 20 plants in the centre of each plot. Plant height was measured using a tall ruler and stem diameter was determined with a digital Vernier calliper according to Stanschewski *et al.* (2021). Achene yield per plant (g/pl), achene yield (kg/ha) and 1000 achene weight (g) were determined at harvest 160 days after sowing. Specific leaf area (SLA) was calculated as the ratio of leaf area (measured with a leaf area meter LICOR LI-3100C) to leaf dry mass (cm^2/g). Leaf dry mass was determined by drying the tissue at 55°C until constant weight was reached. Phosphorous content of the leaves was estimated by the molybdate method (Murphy and Riley, 1962), whereas the leaf and achene nitrogen content were quantified by the micro-Kjeldahl method with colorimetric ammonium (NH_4^+) determination (Nkonge and Ballance, 1982). Total protein content was calculated from the nitrogen content using a conversion factor of 6.25.

Anatomical and ultrastructural studies, optic (OM) and transmission electron microscopy (TEM)

Undamaged leaves, without visual effects of pests or diseases, from the fourth node of three individuals of each treatment (LD and HD) sown in the central furrow were selected. Pieces of leaf tissue of approximately 1 mm^2 were fixed for 4 h at 4°C in 5% glutaraldehyde (0.1 M phosphate buffer, pH 7.4) for histological and ultrastructural analysis, while the rest of the leaf was

fixed in FAA (formalin:ethanol:acetic acid:water; 100:500:50:350, v/v) (Johansen, 1940) at room temperature during 24 h.

Leaf sections of approximately 1 cm² of the samples fixed in FAA were diaphanized following the Dizeo de Strittmatter (1973) technique, subsequently they were stained with cresyl violet 1% in distilled water and mounted in 50% glycerol for epidermal analyses.

For histological and ultrastructural analysis, the samples fixed in glutaraldehyde were post-fixed in 1% OsO₄ (0.1 M phosphate buffer, pH 7.4) for 60 min, dehydrated in a graded ethanol series followed by an ethanol-acetone series and embedded in Spurr's resin (Sigma-Aldrich, St. Louis, MO, USA). Semi-thin sections (1 µm thick) and ultra-thin sections were cut on an ultramicrotome using a diamond knife and mounted on glass slides. Semi-thin sections were stained with 0.5% toluidine blue O (Sigma-Aldrich) in aqueous solution and analysed in a Karl Zeiss Axiostar plus optical microscope. The pictures were taken with a coupled digital camera Axio Cam ERc 5S Zeiss using the AxioVision Rel.4.3 software.

Ultra-thin sections were stained in uranyl acetate followed by lead citrate (EMS, Hatfield, PA, USA), and examined in a TEM LIBRA 120 (Carl Zeiss) transmission electron microscope at the Electron Microscopy Research and Services Center (CISME, CONICET-UNT).

Stomata density (SD) was calculated estimating number of stomata/unit of area and stomata index (SI) was estimated as:

$$SI = \left[\frac{\text{number of stomata}}{(\text{number of epidermal cell} + \text{number of stomata})} \right] \times 100 \quad (1)$$

within a unit of area. In cross-sections the number of cells per unit area (mm²) for adaxial palisade (AdPc), spongy mesophyll (SMc) and abaxial palisade (AbPc) layers was determined. The total cross-sectional area of mesophyll tissues without the epidermis (M), the intercellular airspaces area (Ias), the mesophyll area occupied by mesophyll cells (Mce) and by vascular bundle tissues (Vb) considering their parenchyma sheath as part of the structure were measured. The thickness of each tissue (epidermis, adaxial palisade, spongy and abaxial palisade mesophyll) and the total length of the analysed leaf cross section (L) were measured in light microscope images at 200× magnification.

The total length of the mesophyll cell wall exposed to the intercellular air space (Im) and the total length of the chloroplasts touching the plasma membrane appressed to the intercellular air space (lc) were calculated in light and electron microscope images respectively (Xiong *et al.*, 2017). Mesophyll surface area exposed to intercellular air spaces per leaf area (Sm) and chloroplast surface area exposed to intercellular airspaces per leaf area (Sc) were calculated from light and electron micrograph respectively as follows:

$$Sm = Im/F \quad (2)$$

$$Sc = \frac{lc}{Im} \times Sm \quad (3)$$

where F is the curvature correction factor to convert the length in cross-sections to a surface area. F was measured and calculated for each treatment as 1.35 for LD and 1.40 for HD (Thain, 1983) with

modification suggested by Evans *et al.* (1994). The thickness of the cell wall (Tcw), cytoplasm (Tcyt), chloroplast stroma (Tstr) and the chloroplast area (Ca) were measured from electron micrographs. Chloroplast thickness (Cthi) as a restriction to CO₂ penetration was approximated according to Evans *et al.* (1994) as:

$$Cthi = Ca/lc \quad (4)$$

Also, the number of chloroplasts (Cnum) per adaxial palisade cell unit was measured. The average value of ten measurements of each quantified parameter per leaf (*n* = 3 leaf blades per treatment) was informed. For chloroplast parameters, three palisade cells from each repetition and three chloroplasts of the adaxial palisade mesophyll per leaf were evaluated.

The *Image J* software (National Institute of Health, Bethesda, MD, USA) and AxioVision Rel.4.3 software were used.

Gas exchange

Gas exchange measurements were performed on a sunny day using an open infrared gas analyser (IRGA-6400 XT) equipped with a fluorometer chamber (LI-COR 6400 XT, LI-COR, Lincoln, NE, USA). All measurements were performed on the third uppermost fully expanded leaves located in the main stem at the beginning of flowering stage. The *A*_{max} (net CO₂ assimilation rate under conditions of light and CO₂ saturation) estimation was made under constant leaf temperature (usually 25 ± 1°C), photosynthetic photon flux density (PPFD, 1500 µmol/m²/s) and CO₂ concentration of 400 µmol CO₂/mol air according to Geissler *et al.* (2015) and provided by the LI-COR equipment, after a 3–5 min acclimation period.

All measurements were made at a RH of 50–60% and air flow rate of 500 µmol/s. Each measurement was repeated until obtaining at least three stable values in five different plants. All measurements were made from 09:30 to 12:30 am. The carboxylation capacity and maximum carboxylation capacity were expressed as *A_n/C_i* and *A_{max}/C_i* ratios whereas the instantaneous water use efficiency (_iWUE) was calculated as *A_{max}/g_s* ratio (Rawson *et al.*, 1977). Light compensation point (LCP), light saturation point (LSP), dark respiration rate (*R_d*) and apparent quantum yield of photosynthetic CO₂ assimilation (_φCO₂) were calculated from photosynthetic light response curves (An/PPFD curves). The curves were fit according to an exponential function described by Schulte *et al.* (2003) using the following equation:

$$Y = a - (\exp(-b \times X)) \times c \quad (5)$$

where Y = An, X = PPFD and *a*, *b* and *c* are the calculated parameters. Photosynthetic photon flux densities (PPFD) ranged between 0 and 2500 µmol/m²/s were used.

Pigment contents

Plants used for gas exchange measurements were also used to determine both photosynthetic (chlorophylls and carotenoids) and UV-B absorbing pigments (protective pigments). Chlorophyll and carotenoids were extracted using dimethyl sulfoxide during 12 h in darkness at 45°C, as described by Chappelle *et al.* (1992). Chlorophyll *a*, *b* and carotenoids contents were calculated from absorbances at 649, 665 and 480 nm according to Wellburn's procedure (1994) and expressed as mg/g DW. UV-B absorbing compounds were extracted using acidified methanol:water:HCl,

Table 1. Achene yield, morphological parameters, N and P leaf mineral content for low-density (LD) and high-density (HD) planting treatments

	LD	HD
Achene yield (kg/ha)	5383 ± 434a	2520 ± 230b
Achene protein content (%)	15.0 ± 1.5a	11.3 ± 0.9b
1000 achene weight (g)	2.69 ± 0.20a	2.28 ± 0.14b
Plant height (m)	2.2 ± 0.1a	1.7 ± 0.1b
Stem diameter (cm)	2.2 ± 0.2a	0.9 ± 0.2b
SLA (cm ² /g)	115.8 ± 11.0a	189.8 ± 15.8b
Leaf N content (mmol/m ²)	103.1 ± 9.2a	79.0 ± 5.2b
Leaf P content (mmol/m ²)	3.9 ± 0.5a	2.9 ± 0.4b

Data are the means and standard deviation. Plant height and stem diameter is a mean of 20 different plants. All the others are mean of three plants. SLA, specific leaf area. Different letters indicate significant differences calculated for $P \leq 0.05$.

79:20:1 according to the procedure of Mirecki and Teramura (1984) determined spectrophotometrically at 305 nm and expressed as $\text{Abs}_{305}/\text{mg DW}$.

Statistical analysis

Data were evaluated for homogeneity of variance using Tukey test. The mean values between treatments were compared using the *t*-test at $P \leq 0.05$ level of probability (statistical package SPSS Inc., version 11.0, Chicago, IL, USA).

Results

The following results correspond to averaged data from 2018/2019 and 2019/2020 cropping cycles. It is worth noting that for the first analysis, year was considered as a factor, notwithstanding, no differences between years were found, thus only results for density treatments were analysed. The study site has a desert type climate, the trials were conducted in similar dates between years under irrigation, and no differences in temperature and radiation were registered, explaining the absence of significant differences between years.

Achene yield and morphological parameters

HD treatment showed a decrease of 2863 kg/ha, 4 g/100 g DW, 0.41 g, 0.5 m, 1.3 cm on achene yield, protein content, 1000-achene weight, plant height and stem diameter respectively, when compared to LD. On the contrary SLA was higher in HD compared to LD (Table 1).

Leaf nitrogen and phosphorus content

Leaf N and P content in quinoa were affected by plant density. A significant decrease was found in HD in relation to LD, with a reduction of 24.1 mmol/m² for N and 1 mmol/m² for P (Table 1).

Leaf morphological and anatomical parameters

The general morphological characteristics of the leaves were identical in both treatments. *Chenopodium quinoa* var CICA-17 showed simple notophyll triangular leaves with long, fine and furrowed petioles. Ovate symmetrical lamina with the wider region at

the base. The base was truncate obtuse with rounded obtuse apex and dentate to crenate margin. In superficial view quinoa leaves were amphistomatic as informed by González *et al.* (2014). Anomocytic stomata types and epidermal bladder cells were observed on both leaf surfaces. Adaxial epidermal cells were isodiametric with slightly curved anticlinal cell walls while abaxial cells presented slightly sinuous anticlinal walls. Stomata densities and index were different ($P \leq 0.05$) in both epidermis predominating in the abaxial epidermis (Table 2) and also were affected by plant density treatments, both parameters showed significant differences particularly in the abaxial epidermis, displaying lower densities and indexes in HD compared to LD (Table 2). Total SD (upper epidermis + lower epidermis) decreased from 396 stomata/mm² under LD to 215 stomata/mm² in HD. The length of the occlusive cells was slightly mayor at HD treatment probably compensating the minor density observed (Table 2).

Cross-sections of both assayed treatments showed smooth cuticle and monostratified epidermis with slightly sunken stomata on both epidermal surfaces (Figs 1(a) and (b)). The mesophyll showed heterogeneous isolateral mesophyll with adaxial palisade parenchyma with 2–3 strata, irregular spongy central parenchyma loosely arranged and one abaxial strata of palisade with shorter loosely arranged cells with respect to adaxial palisade. Minor collateral vascular bundles were surrounded by a one-layered parenchyma sheath. Crystaliferous idioblast with calcium oxalate druses were observed without differences among the treatments (Figs 1(a) and (b), Table 3).

Both treatments showed similar characteristics regarding the distribution and the number of strata of the mesophyll tissues, but exhibited quantitative differences. The values obtained for tissue thicknesses for LD and HD were very similar, however, the thickness of the leaf blade and the adaxial palisade parenchyma exhibited significantly higher values for LD than for HD (Tables 3 and 4). Similarly, a major leaf section, mesophyll area (M) and mesophyll area occupied by cells (Mce) were observed in LD, only ascribable to a greater development of adaxial palisade cells (Tables 2 and 3). However, this increase was not reflected in the proportion of intercellular spaces (Ias) or in the mesophyll surface area exposed to intercellular air spaces per leaf area (Sm), values that did not show significant differences between treatments (Table 4).

Ultrastructurally the chloroplasts showed starch grains and plastoglobuli in their stroma; and grana thylakoids showed a well-developed structure. The number and size of starch grains and plastoglobuli were similar in both treatments (Figs 1(c) and (d)). HD treatment showed a higher number of chloroplasts per palisade cell with respect to LD, perhaps as a compensatory mechanism for the decrease observed in the stomata densities and the size of the palisade cells (Table 5). Although the dimensions of the chloroplasts, total length of the chloroplasts touching the plasma membrane appressed to the intercellular air space (lc) and chloroplast surface exposed to intercellular airspaces per leaf area (Sc) did not present significant differences in both treatments, HD treatment showed an increasing trend in chloroplast thickness (Cthi) with higher values of cytoplasm thickness (TCyt), cell wall thickness (Tcw) and chloroplast stroma thickness (Tstr) constituting a barrier of restriction to CO₂ penetration (Table 5). It was interesting to observe that in HD some chloroplasts appeared overlap and compress, on this last case resulting in the separation between the plastid membrane and the cell wall (Figs 1(e) and (f)).

Table 2. Stomata density (SD), stomata index (SI) and stomata dimensions in low-density (LD) and high-density (HD) planting treatments

	SD (Stomata/mm ²)	SI	Stomata length (μm)					
			Adaxial epidermis			Abaxial epidermis		
				Latitude	Longitude		Latitude	Longitude
LD	161.9 ± 26.2a	233.9 ± 41.4a	17.2 ± 1.5a	20.4 ± 0.8a	21.2 ± 1.0a	16.5 ± 0.8b	21.4 ± 1.5b	17.3 ± 0.9b
HD	98.1 ± 10.8b	116.7 ± 16.3b	16.5 ± 1.0a	18.1 ± 1.7b	24.3 ± 1.7a	19.2 ± 1.6a	25.5 ± 1.0a	21.6 ± 1.5a

Data are expressed as mean and standard deviation of ten measurements of each quantified parameter per leaf ($n = 3$ leaf blades per treatments). Different letters indicate significant differences calculated for $P \leq 0.05$.

Photosynthetic pigment content

In the current study a significant difference ($P \leq 0.05$) was found in all photosynthetic (chlorophylls and carotenoids) and protective pigments, with higher contents for LD compared to HD (Table 6).

Maximal photosynthetic assimilation

Under light and CO₂ saturating conditions (1500 μmol/m²/s¹ and 400 μmol/mol) the maximal photosynthetic rate (A_{max}) decreased about 7.3 μmol/m²/s under HD in relation to LD, while the stomata conductance (g_s) showed a decrease of 0.053 mol/m²/s. Carboxylation capacity showed a significant difference ($P \leq 0.01$) with an increment of 73 mmol/m²/s at LD respective to HD while iWUE did not show any difference (Table 7).

Effect of different plant densities on CO₂ assimilation under different light intensities (An/PPFD curves)

The An/PPFD curves are shown in Fig. 2. The A_{max} values for LD and HD were 36.6 and 28.7 μmol CO₂/m²/s respectively (Table 5). The intensities at which light saturation was reached were significantly different between LD and HD. CO₂ assimilation saturated at 1265 PAR/μm²/s in LD and at 1012 μmol PAR/m²/s in HD (Table 8). Light compensation point (LCP), apparent quantum yield of photosynthetic CO₂ assimilation (ϕ_{CO_2}) and dark respiration rate (R_d) did not show significant differences between LD and HD.

Discussion

It is well known that plant responses to different stress involve diverse mechanisms at different levels, like molecular, biochemical, physiological processes and different morphological and developmental adjustments (Munns, 2002). Quinoa, with a large latitudinal and altitudinal distribution in the Andes mountain, has different ecotypes (from sea level to high mountains) (Tapia, 2015) which implies a great plasticity undoubtedly related to their genetic constitution (Fuentes *et al.*, 2012; Jarvis *et al.*, 2017).

A complex topic to address for this and many other cultivated species is the effect of plant densities on yield. Generally, most studies are focused on the plant density effect on yield components (i.e. achene number and size), but understanding physiological, morphological and anatomical responses to increased plant density are needed for taking agronomical management decisions and for enhancing resources use efficiencies.

In this experiment, we demonstrated that under the same growing conditions (insolation regime, soil type, watering regime and agronomical management) and without visual effects of water or nutrients stress, the increase of light competition mediated by a higher plant density triggered responses at morphological, anatomical and physiological levels. Although these changes allowed the quinoa crop to cope with the enormous light stress imposed by the high density of plants, a penalty in yield was registered.

Regarding SLA, it is a very sensible parameter to evaluate responses to stress conditions or different treatments (Lambers *et al.*, 1998) and it has a strong relation with leaf thickness, leaf nitrogen content and photosynthetic assimilation (Evans, 1989; Garnier *et al.*, 1997; Evans and Poorter, 2001; Croft *et al.*, 2017). In our study, the cost in carbon to achieve 1 cm² of leaf (specific leaf mass = 1/SLA) was 6.42 and 5.27 mg D.W./m² for

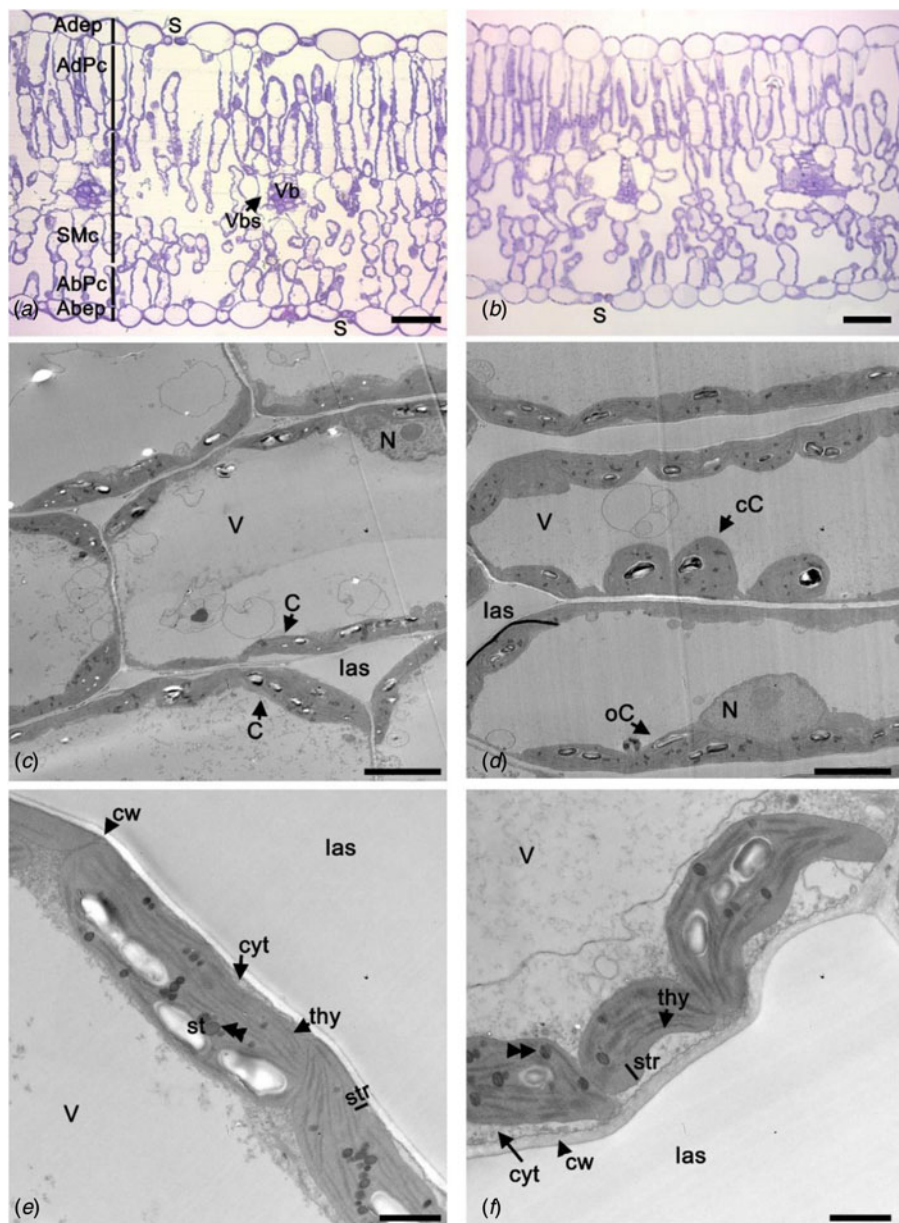


Fig. 1. Colour online. *Chenopodium quinoa* Var. CICA. (a, c, e) Low-density sowing (LD) treatment, (b, d, f) high-density sowing (HD) treatment. (a, b) Leaf transection, optic microscopy. (d-f) Cell and chloroplast at TEM. Scales A-B, 50 µm; C-D, 5 µm; E-F, 1 µm. Abbreviations: Abep, abaxial epidermis; AbPc, abaxial palisade cells; Adepc, adaxial epidermis cells; AdP, adaxial palisade; ccC, compress chloroplast; C, chloroplast; cw, cell wall; cyt, cytoplasm; double arrow head, plastoglobuli; las, intercellular air spaces; N, nucleus; oC, overlap chloroplasts; S, stomata; SMC, spongy mesophyll cells; st, starch; thy, thylakoids; V, vacuole; Vb, vascular bundle; Vbs, vascular bundle parenchyma sheath.

LD and HD, respectively. This significant difference shows that under HD quinoa leaves presented a lower carbon investment and it was highly correlated with the leaves thickness. Under HD, the leaves thickness was sensibly less than under LD. The increase of leaves thickness under LD was attributed to the formation of longer palisade cells in the mesophyll and to the development of multiple palisade parenchyma on both sides of the leaf.

In relation to leaf anatomy, there is huge evidence of the effect of sunlight on the tissue's arrangements (Karabourniotis *et al.*, 2021). In our study, the development of different SLA, stomata densities, indexes and dimensions, the differences observed at the length of the palisade cells and the chloroplast arrangement within the cells were the most evident affected parameters comparing both treatments. According to several researchers (Vogelmann and Martin, 1993; Brodersen *et al.*, 2007) these arrangements facilitate light channelling into the leaf. In relation to the total thickness of the leaf, the spongy parenchyma, with irregularly cells, was slightly increased, although not significantly,

under HD treatments, probably as an adaptation of the leaves to form a large intercellular air spaces to enhance gas and light absorption due to multiple light scattering (Evans and Vogelmann, 2003). According to Vogelmann (1989) and DeLucía *et al.* (1996) the spongy mesophyll is an adaptation to enhance leaf absorptance in shade leaves by the increasing of the internal light scattering which improves the probability of absorption for photosynthesis. Therefore, a greater proportion of spongy mesophyll under HD may be a response to the light stress in an attempt to cope with it, trying to maintain its photosynthetic assimilation. However, photosynthetic rate was about 7.3 µmol/m²/s lower in HD compared to LD, showing a lack of adaptation to the HD studied.

Other important elements in the gas exchange process are the stomata densities (SD) and indexes (SI). Stomata play a crucial role in the CO₂ capture and transpiration. Our analysis showed that total SD (lower + upper epidermis) was higher in LD compared to HD. Notwithstanding as a compensation strategy, the

Table 3. Leaf tissues thickness and area for low-density (LD) and high-density (HD) planting treatments

Adaxial epidermis	Adaxial palisade parenchyma			Spongy parenchyma			Abaxial palisade parenchyma			Leaf blade thickness (μm)
	Thickness (μm)	Thickness (μm)	AdPc/mm ²	Thickness (μm)	SMc/mm ²	Thickness (μm)	AbPc/mm ²	Thickness (μm)	Crystal idioblast /mm ²	
LD	24.8 ± 4.6a	117.3 ± 16.6a	292.3 ± 7.9a	96.1 ± 16.5a	310.7 ± 44.9a	39.9 ± 19.2a	129.0 ± 16.4a	21.0 ± 5.41a	7.4 ± 3.5a	299.2 ± 21.6a
HD	23.7 ± 5.1a	101.4 ± 12.8b	320.2 ± 29.3a	102.4 ± 12.9a	357.9 ± 41.5a	33.4 ± 5.7a	102.2 ± 33.3a	20.3 ± 3.91a	7.1 ± 6.8a	281.2 ± 7.8b

Data are expressed as mean of ten measurements of each quantified parameter per leaf ($n=3$ leaves per treatment) and standard deviation. Different letters indicate significant differences calculated for Tukey $P \leq 0.05$. References: AdPc/mm², adaxial palisade cells/mm²; SMc/mm², spongy mesophyll cells/mm²; AbPc/mm², abaxial palisade cells/mm².

stomata size was greater in HD. Also, the SD has a deep relationship with plant water status. In fact, according to our data the decrease in SD in plants growing under HD compared to LD, contributed to a decrease of 0.053 mol/m²/s in g_s and 1.65 mmol/m²/s in E . This reduction in transpiration and stomata conductance contributed to the lower yield obtained in HD.

In quinoa leaves or cotyledons the presence of calcium or carbonate oxalate is common (Prado *et al.*, 2017) and usually calcium is accumulated in crystalliferous idioblast. These ergastic components together with silicon have been proposed as elements for improving light scattering within the mesophyll (Bauer *et al.*, 2011; He *et al.*, 2014). Although we detected the presence of idioblasts, no significant differences were found among treatments. Thus, in this case the presence of crystalliferous idioblasts with carbon oxalate druses did not play a role in light scattering, probably displaying another function like providing protection against photo-inhibition or moderating internal leaf temperature (Horner *et al.*, 2017). It is worth noting that in the extreme environment where the experiment was carried out, moderating internal leaf temperature is a very important issue due to high temperatures and radiation that are registered during the day (González *et al.*, 2011).

Chloroplasts are very important organelles in plants because they are the sites where photosynthesis is performed. Chloroplast morphology can adapt to different environments and light conditions affecting their structures, ultrastructure and function in the photosynthesis process (Franklin and Whitelam, 2004). It is well known that chloroplasts are more susceptible to damage by different abiotic stresses (Molas, 2002). Some stresses like saline can destroy the chloroplast organization even in quinoa (Bose *et al.*, 2017; Manaa *et al.*, 2019). In relation to light competition effect, our results demonstrated that chloroplast has maintained the structural organization with some little changes that allowed plant to conserve the function. In general, the ultrastructure of the chloroplasts under LD and HD showed a fully developed grana with many layers, starch and some plastoglobuli. The higher number of chloroplasts per palisade cell observed at HD treatment in relation to LD may be interpreted as an attempt to compensate the decrease observed in the size of these cells. HD treatment showed increasing trend in the cell wall, cytoplasm, chloroplast and chloroplast stroma thickness, constituting restriction barriers to CO₂ penetration.

In the present study the differences of total chlorophylls, carotenoids and protective pigments under LD and HD may be explained by the different levels of radiation that leaves were exposed and the lesser thickness of the mesophyll observed in HD. Plants under HD treatment reduced its chlorophyll content about 11% compared to LD. This may be an indicator of stress linked to competence by different resources. The Chl.*a*/Chl.*b* ratio reflected the higher light exposition of leaves under LD than in HD. In addition, the ratio of chlorophyll *a* to *b* in land plants has been used widely as an indicator of response to shade and as an early indicator of senescence.

In the case of carotenoids, these pigments play an important role in light harvesting complexes and in photo-protection of the photosystems (Hendry and Price, 1993). In CICA-17 under HD carotenoids increased about 0.13 mg/gDW as compared to LD, probably as a strategy for light harvesting complex under the shadow caused by other plants and leaves. Similarly, an increase was observed in the total chlorophyll/carotenoids ratio. The differences in solar radiation that leaves from LD and HD received were reflected in the absorbance at 305 nm (protective

Table 4. Mesophyll anatomical characteristics associated with resistance to gas diffusion for low-density (LD) and high-density (HD) treatments

	Lm (μm)	Sm	M (μm^2)	las (μm^2)	Vb (μm^2)	Mce (μm^2)
LD	7178.2 \pm 153.6a	21.7 \pm 0.5a	114 619.1 \pm 3606.1a	41 847.9 \pm 4472.4a	7873.9 \pm 1639.5a	64 897.3 \pm 2250.8a
HD	7073.1 \pm 680.4a	22.2 \pm 2.4a	106 820.6 \pm 2199.1b	41 266.9 \pm 2610.8a	8775.3 \pm 2140.5a	56 778.4 \pm 1751.4b

Data are expressed as mean and standard deviation. Different letters indicate significant differences calculated for Tukey $P \leq 0.05$. References: Lm, length of the mesophyll cell wall exposed to the intercellular air space; Sm, mesophyll surface area exposed to intercellular air spaces per leaf area; M, mesophyll area; las, intercellular airspace area; Vb, vascular bundles total area per section; Mce, mesophyll area occupied by parenchyma cells without vascular bundles with their respective parenchyma sheaths.

Table 5. Cell wall and chloroplast anatomical characteristics associated with resistance to gas diffusion for low-density (LD) and high-density (HD) planting treatments

	Lc (μm)	Sc	Cthi (μm)	Ca (μm^2)	Cnum	Tcw (μm)	TCyt (μm)	Tstr (μm)
LD	4.5 \pm 0.6a	0.013 \pm 0.002a	1.36 \pm 0.07a	6.05 \pm 0.52a	16.00 \pm 2.00b	0.11 \pm 0.03b	0.09 \pm 0.06b	0.14 \pm 0.05b
HD	4.3 \pm 0.4a	0.013 \pm 0.001a	1.60 \pm 0.25a	6.85 \pm 1.40a	21.33 \pm 1.53a	0.21 \pm 0.11a	0.13 \pm 0.10a	0.22 \pm 0.13a

Data are expressed as mean and standard deviation. Different letters indicate significant differences calculated for Tukey $P \leq 0.05$. References: Lc, total length of the chloroplasts touching the plasma membrane appressed to the intercellular air space; Sc, chloroplast surface exposed to intercellular airspaces per leaf area; Cthi, chloroplast thickness as restriction to CO₂ penetration; Ca, Chloroplast area; Cnum, chloroplast number per adaxial palisade cell; Tcw, cell wall thickness; TCyt, cytoplasm thickness; Tstr, chloroplast stroma thickness.

Table 6. Leaf photosynthetic pigments content for low-density (LD) and high-density (HD) treatments

	Chl. a (mg/g DW)	Chl. B (mg/g DW)	Chl. a + b (mg/g DW)	Chl. a/Chl.b	Carot. (mg/g DW)	Chl. a + Chl b /Carot.	Abs. ₃₀₅ /g DW
LD	3.39 \pm 0.14a	0.72 \pm 0.09a	4.11 \pm 0.12a	4.73 \pm 0.07a	0.63 \pm 0.03b	6.56 \pm 0.21a	0.37 \pm 0.01a
HD	3.01 \pm 0.08b	0.67 \pm 0.02b	3.68 \pm 0.1b	4.53 \pm 0.11b	0.76 \pm 0.03a	4.83 \pm 0.29b	0.26 \pm 0.03b

Data are expressed as mean and standard deviation. Different letters indicate significant differences calculated for Tukey $P \leq 0.05$. References: Carot, carotenoids; Chl, chlorophyll; DW, dry weight.

Table 7. Physiological-photosynthetic parameters evaluated for low-density (LD) and high-density (HD) treatments under light and CO₂ saturation conditions

	A_{\max} $\mu\text{mol/m}^2/\text{s}$	g_s $\text{mol/m}^2/\text{s}$	C_i $\mu\text{mol CO}_2/\text{mol}$	E $\text{mmol/m}^2/\text{s}$	A_{\max}/C_i $\text{mmol/m}^2/\text{s}$	WUE_{i} $\mu\text{mol/mol}$
LD	34.3 \pm 2.3a	0.238 \pm 0.03a	141.4 \pm 7.2a	7.83 \pm 0.66a	242.6 \pm 20.3a	144.1 \pm 9.4a
HD	27.0 \pm 1.9b	0.185 \pm 0.01b	159.2 \pm 10.1a	6.18 \pm 0.59b	169.6 \pm 10.5b	156.1 \pm 14.0a

Data are expressed as mean and standard deviation. Different letters indicate significant differences calculated for $P \leq 0.05$. References: A_{\max} , maximal photosynthetic rate; g_s , stomata conductance; C_i , intercellular CO₂ concentration; E, transpiration rate; A_{\max}/C_i , maximum carboxylation capacity; WUE, water use efficiency.

pigments) where the value under LD was 0.11Abs.₃₀₅/g DW higher than in HD. As observed in the present work, leaves developed under shade have higher numbers of thylakoid stacks in the chloroplast but lower chlorophyll contents and net photosynthesis rates than leaves developed under normal light conditions (Marchiori *et al.*, 2014).

The gas exchange measurements showed that A_{\max} was affected by plant densities where the highest A_{\max} was detected in LD treatment. A_{\max} in quinoa can vary according to different genotypes and agronomical managements among another parameters (González *et al.*, 2011). The A_{\max} value obtained under light and CO₂ saturation conditions were in the range of those previously informed for CICA-17 growing in the same field where this study was performed. González *et al.* (2011) reported a value of 31 $\mu\text{mol/m}^2/\text{s}$ while in our study we found values of 34.3 and 27.0 $\mu\text{mol/m}^2/\text{s}$ for LD and HD respectively. The A_{\max} decrease in our study had a strong relationship with leaves nitrogen and

total chlorophyll content. It is known that there exists a strong and positive correlation between leaves nitrogen and photosynthesis considering that nitrogen has an important role in the Calvin cycle enzymes (Evans, 1989). Ribulose-1,5-biphosphate carboxylase/oxygenase represents nearly 50% of all the total leaf protein (Lambers *et al.*, 1998).

From the light response curve (A_n/PPFD) we can establish that LSP was different in LD compared to HD. This fact could be directly related to the different degree of leaves insolation as happens in sun or shades leaves. In relation to the LCP, R_d and quantum yield of photosynthetic CO₂ assimilation (ϕCO_2), no significant differences were detected, which is to be expected since these are species-specific variables (Valladares *et al.*, 1997).

The most evident characters modified by light allocation caused by plant densities were plant height, stem diameter; leaf specific area, thickness, chloroplast ultrastructure; nitrogen, phosphorous and pigments (photosynthetic and protective) content.

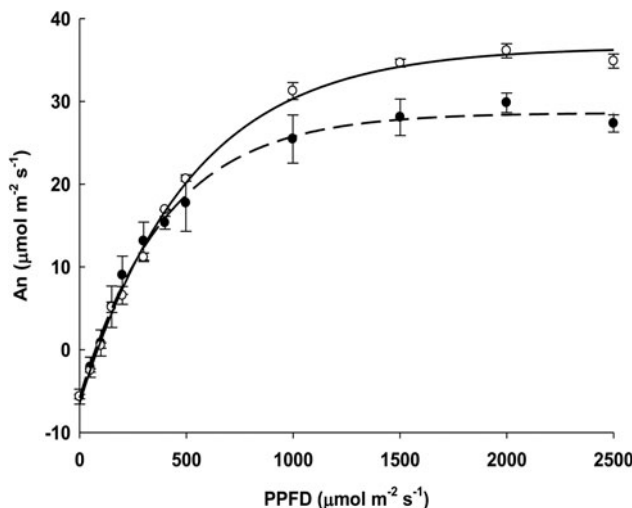


Fig. 2. Net CO_2 assimilation rate (An) as a function of the photosynthetic photon flux density (PPFD). (○, —) Low density; (●, ----) high density. Each point is the mean \pm SD of five independent measurements. Vertical bars indicate SD.

Data obtained in this work allow to affirm that although quinoa crop showed morphological and anatomical changes in an attempt to reduce the light competition generated by high-density treatment, these changes did not fully compensate gas exchange, limiting C absorption and therefore limiting uptake of N and P, resulting in a lower yield of HD compared to LD. Considering the ability of quinoa plants to change its morphology and anatomy, further studies with intermediate plant densities are needed in order to determine if it is possible to achieve higher yields than those obtained with the low density studied here.

In order to get a wider knowledge about how light allocation and plant density may affect quinoa production, it is necessary to investigate different quinoa ecotypes at different plant densities under different sunlight conditions to establish the best density for each ecotype and for each place where quinoa may be an important complementary crop.

Conclusion

Plant density treatment affected quinoa yield by altering photosynthesis physiology, pigments accumulation, plant morphology and leaf anatomy and ultrastructure. Different achene yield under LD and HD was a direct consequence of differences in photosynthetic assimilation and morpho-anatomical modifications caused by light competition induced by plants and leaves shading. This work constitutes a first approximation to understand the phenotypic plasticity of quinoa against different light competition levels caused by contrasting plant densities.

Table 8. Photosynthetic parameters calculated from photosynthetic light response curves (An/PPFD curves) evaluated for low-density (LD) and high-density (HD) treatments

	A_{\max} ($\mu\text{mol/m}^2/\text{s}$)	LSP ($\mu\text{mol/m}^2/\text{s}$)	LCP ($\mu\text{mol/m}^2/\text{s}$)	ϕCO_2 (mol/mol)	R_d ($\mu\text{mol/m}^2/\text{s}$)
LD	$36.6 \pm 0.4\text{a}$	$1265.2 \pm 35.8\text{a}$	$83.5 \pm 3.40\text{a}$	$0.071 \pm 0.01\text{a}$	$-6.47 \pm 0.4\text{a}$
HD	$28.7 \pm 1.9\text{b}$	$1012.0 \pm 16.7\text{b}$	$77.2 \pm 4.80\text{a}$	$0.072 \pm 0.02\text{a}$	$-5.80 \pm 0.5\text{a}$

Data are expressed as mean and standard deviation. Different letters indicate significant differences calculated for $P \leq 0.05$. References: A_{\max} , maximal photosynthetic rate; LSP, light saturation point; LCP, light compensation point; ϕCO_2 , apparent quantum yield of photosynthetic CO_2 assimilation; R_d , dark respiration rate.

Acknowledgements. To the technicians of the Campo Experimental de Encalilla – INTA – Amaicha del Valle who helped in field crop work.

Author contributions. JAG, MIM, LEE, LMC, SEB and GIP conceived of the presented idea and planned the experiments. SEB, LMC, DAG and LEE carried out and analysed the data of the field experiments. JAG, SEB and DAG carried out the physiological parameters measurements. MIM and GIP carried out the morpho-anatomical evaluations. All authors supervise the project, discussed the results and contributed to the final manuscript.

Financial support. This work was supported by Miguel Lillo Foundation ('Ecophysiology of selected *Chenopodium quinoa* varieties and other species of nutritional value in field and lab') (Project B-0004-1) and National Institute of Agricultural Technology (INTA) under the project 'Aplicación de tecnología para producción de quinoa para alimentación y generación de un mercado de semillas en la Comunidad Indígena de Amaicha del Valle (Tucumán)'. Consejo Federal de Ciencia y Tecnología (COFECYT). Ministerio de Ciencia, Tecnología e Innovación Productiva (MINCYT). RESOL-2018-680-APN-MCT.

Conflict of interest. None.

Ethical standards. Not applicable.

References

- Abdalla D, Jorge A-B, Abdou G, Amidou G, Louis N and Jacob S (2020) Effect of different planting techniques and sowing density rates on the development of quinoa. *African Journal of Agricultural Research* **16**, 1325–1333.
- Alandia G, Rodriguez JP, Jacobsen SE, Bazile D and Condori B (2020) Global expansion of quinoa and challenges for the Andean region. *Global Food Security* **26**, 100429.
- Andreotti F, Bazile D, Biaggi MC, Callo-Concha D, Jacquet J, Jemal OM, King OI, Mbosso C, Padulosi S, Speelman EN and Van Noordwijk M (2022) When neglected species gain global interest: lessons learned from quinoa's boom and bust for teff and minor millet. *Global Food Security* **32**, 100613. <https://doi.org/10.1016/j.gfs.2022.100613>.
- Angeli V, Miguel Silva P, Crispim Massuela D, Khan MW, Hamar A, Khajehi F, Graeff-Hönninger S and Piatti C (2020) quinoa (*Chenopodium quinoa* Willd.): an overview of the potentials of the 'golden grain' and socio-economic and environmental aspects of its cultivation and marketization. *Foods* **9**, 216.
- Asher A, Galili S, Whitney T and Rubinovich L (2020) The potential of quinoa (*Chenopodium quinoa*) cultivation in Israel as a dual-purpose crop for grain production and livestock feed. *Scientia Horticulturae* **272**, 109534.
- Bauer P, Elbaum R and Weiss IM (2011) Calcium and silicon mineralization in land plants: transport, structure and function. *Plant Science* **180**, 746–756.
- Bazile D, Bertero HD and Nieto C (2015) *State of the Art Report on Quinoa Around the World in 2013*. Santiago du Chili: FAO, CIRAD, 603 p. http://www.fao.org/quinoa-2013/publications/detail/en/item/278923/icode/?no_mobile=1.
- Bazile D, Jacobsen S-E and Verniau A (2016a) The global expansion of quinoa: trends and limits. *Frontiers in Plant Science* **7**, 622.

- Bazile D, Pulvento C, Verniau A, Al-Nusairi M, Ba D, Breidy J, Hassan L, Maarouf IM, Mambetov O, Otambekova M, Sephavand NA, Shams A, Souici D, Miri K and Padulosi S** (2016b) Worldwide evaluations of quinoa: preliminary results from post international year of quinoa FAO projects in nine countries. *Frontiers in Plant Science* **7**, 850.
- Bose J, Munns R, Shabala S, Gilliam M, Pogson B and Tyerman SD** (2017) Chloroplast function and ion regulation in plants growing on saline soils: lessons from halophytes. *Journal of Experimental Botany* **68**, 3129–3143.
- Brodersen CR, Vogelmann TC, Williams WE and Gorton HL** (2007) A new paradigm in leaf-level photosynthesis: direct and diffuse lights are not equal. *Plant Cell and Environment* **31**, 159–164.
- Chappelle EW, Kim MS and McMurtrey JE** (1992) Ratio analysis of reflectance spectra (RARS): an algorithm for the remote estimation of the concentrations of chlorophyll A, chlorophyll B, and carotenoids in soybean leaves. *Remote Sensing of Environment* **39**, 239–247.
- Croft H, Chen JM, Luo X, Bartlett P, Chen B and Staebler RM** (2017) Leaf chlorophyll content as a proxy for leaf photosynthetic capacity. *Global Change Biology* **23**, 3513–3524.
- Cruz Díaz I, Chaparro HN, Díaz LI and Romero Guerrero GA** (2021) Effect of sowing density on the agronomic performance of quinoa Nariño cultivar and the transmissivity of photosynthetically active radiation in the high tropics of Colombia. *Revista Facultad Nacional de Agronomía Medellín* **74**, 9491–9497.
- Delatorre-Herrera J, Ruiz KB and Pinto M** (2021) The importance of non-diffusional factors in determining photosynthesis of two contrasting quinoa ecotypes (*Chenopodium quinoa* Willd.) subjected to salinity conditions. *Plants* **10**, 927.
- DeLucia EH, Nelson K, Vogelmann TC and Smith WK** (1996) Contribution of intercellular reflectance to photosynthesis in shade leaves. *Plant Cell and Environment* **19**, 159–170.
- Dizeo de Strittmatter CD** (1973) Nueva técnica de diafanización. *Boletín de la Sociedad Argentina de Botánica* **1**, 126–129. <https://botanicaargentina.org.ar/wp-content/uploads/2018/09/126-129013.pdf>.
- Eisa SE, El-Samad EH, Hussin SA, Ali EA, Ebrahim M, González JA, Ordano M, Erazzú LE, El-Bordeny NE and Abdel-Ati AA** (2018) Quinoa in Egypt – plant density effects on seed yield and nutritional quality in marginal regions. *Middle East Journal of Applied Sciences* **8**, 515–522. <https://www.cureusweb.com/mejas/mejas/2018/515-522.pdf>.
- El Hazzam K, Hafsa J, Sobeh M, Mhada M, Taourirte M, EL Kacimi K and Yasri A** (2020) An insight into saponins from quinoa (*Chenopodium quinoa* Willd): a review. *Molecules* **25**, 1059.
- Eustis A, Murphy KM and Barrios-Masias FH** (2020) Leaf gas exchange performance of ten Quinoa genotypes under a simulated heat wave. *Plants* **9**, 81.
- Evans JR** (1989) Photosynthesis and nitrogen relationships in leaves of C₃ plants. *Oecologia* **78**, 9–19.
- Evans JR and Poorter H** (2001) Photosynthetic acclimation of plants to growth irradiance: the relative importance of specific leaf area and nitrogen partitioning in maximizing carbon gain. *Plant, Cell & Environment* **24**, 755–767.
- Evans JR and Vogelmann TC** (2003) Profiles of ¹⁴C fixation through spinach leaves in relation to light absorption and photosynthetic capacity. *Plant Cell and Environment* **26**, 547–560.
- Evans J, Caemmerer S, Setchell B and Hudson G** (1994) The relationship between CO₂ transfer conductance and leaf anatomy in transgenic tobacco with a reduced content of RuBisCo. *Functional Plant Biology* **21**, 475–495.
- Feng Y, Lingyang F, Qinlin L, Xiaoling W, Yuanfang F, Muhammad AR, Yajiao C, Junxu C, Xiaochun W, Taiwen Y, Weiguo L, Jiang L, Junbo D, Kai S and Wenyu Y** (2018) Effect of interactions between light intensity and red-to-far-red ratio on the photosynthesis of soybean leaves under shade condition. *Environmental and Experimental Botany* **150**, 79–87.
- Franklin KA and Whitelam GC** (2004) Light signals, phytochromes and cross-talk with other environmental cues. *Journal of Experimental Botany* **55**, 271–276.
- Fuentes F, Bazile D, Bhargava A and Martinez EA** (2012) Implications of farmers' seed exchanges for on-farm conservation of quinoa, as revealed by its genetic diversity in Chile. *Journal of Agricultural Science* **150**, 702–716.
- Garnier E, Cordonnier P, Guillerm J-L and Sonié L** (1997) Specific leaf area and leaf nitrogen concentration in annual and perennial grass species growing in Mediterranean old-fields. *Oecologia* **111**, 490–498.
- Geissler N, Hussin S, El-Far MMM and Koyer H-W** (2015) Elevated atmospheric CO₂ concentration leads to different salt resistance mechanisms in a C₃ (*Chenopodium quinoa*) and a C₄ (*Atriplex nummularia*) halophyte. *Environmental and Experimental Botany* **118**, 67–77.
- González JA, Bruno M, Valoy M and Prado FE** (2011) Genotypic variation of gas exchange parameters and leaf stable carbon and nitrogen isotopes in ten quinoa cultivars grown under drought. *Journal of Agronomy and Crop Science* **197**, 81–93.
- González JA, Ponessa GI, Buedo SE, Mercado MI and Prado FE** (2014) Asimilación fotosintética máxima en variedades de quinoa (*Chenopodium quinoa*) de diferentes orígenes geográficos y su relación con la morfología foliar. *Lilloa* **51**, 177–193. <http://www.lillo.org.ar/revis/lilloa/2014-51-2/06.pdf>.
- González JA, Eisa S, Hussin S and Prado FE** (2015) Quinoa: an Incan crop to face global changes in agriculture. In Murphy KS and Matanguhan J (eds). *Quinoa: Improvement and Sustainable Production*. New Jersey, U.S: John Wiley & Sons, Inc. pp. 1–18.
- González JA, Martín GO, Bruno MA and Prado FE** (2016) La 'quinoa' (*Chenopodium quinoa*) como alternativa forrajera en la zona de los Valles Calchaquíes (Noroeste Argentino). *Lilloa* **53**, 74–81. <http://www.lillo.org.ar/journals/index.php/lilloa/article/view/123>.
- González JA, Jacobsen SE, Buedo SE, Erazzú LE, González DA and Prado FE** (2019) Evaluation of photosynthetic capacity and grain yield of the sea level quinoa variety Titicaca grown in a highland region of Northwest Argentine. *Middle East Journal of Applied Sciences* **09**, 888–900.
- He H, Veneklaas EJ, Kuo J and Lambers H** (2014) Physiological and ecological significance of biominerization in plants. *Trends in Plant Science* **19**, 166–174.
- Heitholt J and Sassenrath-Cole G** (2010) Inter-plant competition: growth responses to plant density and row spacing. In Stewart JM, Oosterhuis DM, Heitholt JJ and Mauney JR (eds). *Physiology of Cotton*. Dordrecht: Springer, pp. 179–186. https://doi.org/10.1007/978-90-481-3195-2_17.
- Hendry GAF and Price AH** (1993) Stress indicators: chlorophylls and carotenoids. In Hendry GAF and Grime JP (eds). *Methods in Comparative Plant Ecology*. London, Chapman Hall, pp. 148–152.
- Hinojosa L, Leguizamo A, Carpio C, Muñoz D, Mestanza C, Ochoa J, Castillo C, Murillo A, Villacréz E, Monar C, Pichazaca N and Murphy K** (2021) Quinoa in Ecuador: recent advances under global expansion. *Plants* **10**, 298.
- Hodgson GL and Blackman GE** (1957) An analysis of the influence of plant density on the growth of *Vicia faba*: II. The significance of competition for light in relation to plant development at different densities. *Journal of Experimental Botany* **8**, 195–219.
- Horner HT, Wanke S, Oelschlägel B and Samain M-S** (2017) Peruvian window-leaved *Peperomia* taxa display unique crystal macropatterns in high-altitude environments. *International Journal of Plant Sciences* **178**, 157–167.
- Jacobsen S-E** (2015) Adaptation and scope for quinoa in northern latitudes of Europe. In Bazile D, Bertero HD and Nieto C (eds). *State of the Art Report on Quinoa Around the World in 2013*. Rome: FAO, pp. 436–446.
- Jacobsen S-E and Christiansen JL** (2016) Some agronomic strategies for organic quinoa (*Chenopodium quinoa* Willd.). *Journal of Agronomy and Crop Science* **202**, 454–463.
- Jacobsen S-E, Jørgensen I and Stølen O** (1994) Cultivation of quinoa (*Chenopodium quinoa*) under temperate climatic conditions in Denmark. *Journal of Agricultural Science* **122**, 47–52.
- Jarvis DE, Ho YS, Lightfoot DJ, Schmöckel SM, Li B, Borm TJA, Ohyanagi H, Mineta K, Michell CT, Saber N, Kharbatia NM, Rupper RR, Sharp AR, Dally N, Boughton BA, Woo YH, Gao G, Schijlen EGWM, Guo X, Momin AA, Negrão S, Al-Babili S, Gehring C, Roessner U, Jung C, Murphy K, Arold ST, Gojobori T, van der Linden C, van Loo EN, Jellen EN, Maughan PJ and Tester M** (2017) The genome of *Chenopodium quinoa*. *Nature* **542**, 307–312.
- Johansen DA** (1940) *Plant Microtechnique*. New York: McGraw-Hill. ed.
- Karabourniotis G, Liakopoulos G, Bresta P and Nikolopoulos D** (2021) The optical properties of leaf structural elements and their contribution to photosynthetic performance and photoprotection. *Plants* **10**, 1455.
- Lambers H, Chapin FS and Pons TL** (1998) *Plant Physiological Ecology*. New York, NY: Springer New York.

- Manaa A, Goussi R, Derbali W, Cantamessa S, Abdelly C and Barbato R** (2019) Salinity tolerance of quinoa (*Chenopodium quinoa* Willd.) as assessed by chloroplast ultrastructure and photosynthetic performance. *Environmental and Experimental Botany* **162**, 103–114.
- Marchiori PER, Machado EC and Ribeiro RV** (2014) Photosynthetic limitations imposed by self-shading in field-grown sugarcane varieties. *Field Crops Research* **155**, 30–37.
- Miltphore FL, Moorby J and González Idiarte H** (1982) *Introducción a la Fisiología de los Cultivos*. Bs.As. Argentina. Hemisferio Sur.
- Mirecki RM and Teramura AH** (1984) Effects of ultraviolet-B irradiance on soybean. *Plant Physiology* **74**, 475–480.
- Molas J** (2002) Changes of chloroplast ultrastructure and total chlorophyll concentration in cabbage leaves caused by excess of organic Ni(II) complexes. *Environmental and Experimental Botany* **47**, 115–126.
- Munns R** (2002) Comparative physiology of salt and water stress. *Plant Cell and Environment* **25**, 239–250.
- Murphy J and Riley JP** (1962) A modified single solution method for the determination of phosphate in natural waters. *Analytica Chimica Acta* **27**, 31–36.
- Nkonge C and Ballance GM** (1982) A sensitive colorimetric procedure for nitrogen determination in micro-Kjeldahl digests. *Journal of Agricultural and Food Chemistry* **30**, 416–420.
- Parwada C, Mandumbu R, Tibugari H, Badze D and Mhungu S** (2020) Effect of soil fertility amendment, planting density and growing season on *Chenopodium quinoa* Willd (Quinoa) in Zimbabwe. *Cogent Food & Agriculture* **6**, 1–16. <https://doi.org/10.1080/23311932.2020.1792668>.
- Prado FE, Hilal MB, Albornoz PL, Gallardo MG and Ruiz VE** (2017) Anatomical and physiological responses of four quinoa cultivars to salinity at seedling stage. *Indian Journal of Science and Technology* **10**, 1–12.
- Rawson HM, Begg JE and Woodward RG** (1977) The effect of atmospheric humidity on photosynthesis, transpiration and water use efficiency of leaves of several plant species. *Planta* **134**, 5–10.
- Rayner M, Sjöök M, Timgren A and Dejmek P** (2012) Quinoa starch granules as stabilizing particles for production of Pickering emulsions. *Faraday Discussions* **158**, 139–155.
- Ren B, Liu W, Zhang J, Dong S, Liu P and Zhao B** (2017) Effects of plant density on the photosynthetic and chloroplast characteristics of maize under high-yielding conditions. *The Science of Nature* **104**, 1–11. <https://doi.org/10.1007/s00114-017-1445-9>.
- Ruiz RA and Bertero HD** (2008) Light interception and radiation use efficiency in temperate quinoa (*Chenopodium quinoa* Willd.) cultivars. *European Journal of Agronomy* **29**, 144–152.
- Ruiz KB, Biondi S, Oses R, Acuña-Rodríguez IS, Antognoni F, Martínez-Mosqueira EA, Coulibaly A, Canahua-Murillo A, Pinto M, Zurita A, Bazile D, Jacobsen SE and Molina Montenegro M** (2014) Quinoa biodiversity and sustainability for food security under climate change. A review. *Agronomy for Sustainable Development* **34**, 349–359.
- Schulte M, Offer C and Hansen U** (2003) Induction of CO₂-gas exchange and electron transport: comparison of dynamic and steady-state responses in *Fagus sylvatica* leaves. *Trees* **17**, 153–163.
- Shabbir A, Abbas G, Asad SA, Razzaq H, Anwar-ul-Haq M and Amjad M** (2021) Effects of arsenite on physiological, biochemical and grain yield attributes of quinoa (*Chenopodium quinoa* Willd.): implications for phytoremediation and health risk assessment. *International Journal of Phytoremediation* **23**, 890–898.
- Shokry AM** (2016) The usage of quinoa flour as a potential ingredient in production of meat burger with functional properties. *Middle East Journal of Applied Sciences* **6**, 1128–1137. <https://www.curesweb.com/mejas/mejas/2016/1128-1137.pdf>.
- Spehar CR and da Silva Rocha JE** (2009) Effect of sowing density on plant growth and development of quinoa, genotype 4.5, in the Brazilian savannah highlands. *Bioscience Journal: BJ* **25**, 53–58. <https://seer.ufu.br/index.php/biosciencejournal/article/view/6952/4608>.
- Stanschewski CS, Rey E, Fiene G, Craine EB, Wellman G, Melino VJ, Patiranage DSR, Johansen K, Schmöckel SM, Bertero HD, Oakey H, Afzal I, Raubach S, Miller N, Streich J, Buchvaldt Amby D, Emrani N, Warmington M, Moussa MAA, Wu D, Jacobson D, Andreasen C, Jung C, Murphy K, Bazile D and Tester M** (2021) Quinoa phenotyping methodologies: an international consensus. *Plants* **10**, 1759, 1–52. <https://doi.org/10.3390/plants10091759>.
- Tapia M** (2015) The long journey of quinoa: who wrote its history. In Bazile D, Bertero HD and Nieto C (eds). *State of the Art Report on Quinoa around the World in 2013*. Rome: FAO, pp. 3–9.
- Thain JF** (1983) Curvature correction factors in the measurement of cell surface areas in plant tissues. *Journal of Experimental Botany* **34**, 87–94.
- Thomas EC and Lavkulich LM** (2015) Community considerations for quinoa production in the urban environment. *Canadian Journal of Plant Science* **95**, 397–404.
- Valladares F, Allen MT and Pearcy RW** (1997) Photosynthetic responses to dynamic light under field conditions in six tropical rainforest shrubs occurring along a light gradient. *Oecologia* **111**, 505–514.
- Van Kleunen M, Stephan MA and Schmid B** (2006) [CO₂]- and density-dependent competition between grassland species. *Global Change Biology* **12**, 2175–2186.
- Villalobos FJ, Sadras VO and Fereres E** (2016) Plant density and competition. In Villalobos F and Fereres E (eds). *Principles of Agronomy for Sustainable Agriculture*. Cham: Springer, pp. 159–168. https://doi.org/10.1007/978-3-319-46116-8_12.
- Vogelmann T** (1989) Penetration of light into plants. *Photochemistry and Photobiology* **50**, 895–902.
- Vogelmann TC and Martin G** (1993) The functional significance of palisade tissue: penetration of directional versus diffuse light. *Plant Cell and Environment* **16**, 65–72.
- Wellburn AR** (1994) The Spectral determination of chlorophylls a and b, as well as total carotenoids, using various solvents with spectrophotometers of different resolution. *Journal of Plant Physiology* **144**, 307–313.
- Xiong D, Huang J, Peng S and Li Y** (2017) A few enlarged chloroplasts are less efficient in photosynthesis than a large population of small chloroplasts in *Arabidopsis Thaliana*. *Scientific Reports* **7**, 5782.